Supporting Information

Bioinspired functional self-healing hydrogels from a minimalistic dipeptide building block

Ipsita Sahu,[a] Yiming Tang,[b] Zichao Wang,[b] Souvik Naskar,[a] Thangavel Vijayakanth,[c] Vivek Vishwanath Adole,[a] Guanghong Wei,[b,] and Priyadarshi Chakraborty [a,*]*

[a]Department of Chemistry
Indian Institute of Technology Hyderabad
Kandi, Sangareddy 502284, Telangana, India
E-mail: priyadarshi@chy.iith.ac.in

[b]Department of Physics
State Key Laboratory of Surface Physics
Key Laboratory for Computational Physical Sciences (MOE)
Fudan University
Shanghai 200433, P. R. China

[c]School of Molecular Cell Biology and Biotechnology,
George S. Wise Faculty of Life Sciences,
Tel Aviv University, Tel Aviv 6997801, Israel

Experimental section

Preparation of the peptide hydrogel. Fmoc-Lys(Fmoc)-Phe was purchased from GL Biochem, Shanghai. Fmoc-Lys(Fmoc)-Phe hydrogel was prepared by solvent switch technique. The peptide was dissolved in DMSO at a concentration of 70 mg mL^{-1}. Then the stock solution was diluted with milli-Q water to get the hydrogels/assemblies.

Preparation of GO-based composite hydrogel. 5 mg of GO (15-20 sheets, 4-10% edge-oxidized, ACS reagent, Sigma-Aldrich) was dispersed in 1 mL of water by ultrasonication. The Fmoc-Lys(Fmoc)-Phe stock solution was diluted with required quantities of milli-Q water and GO dispersion, yielding the peptide/GO composite hydrogel. The final GO concentration in the hydrogel was 0.5% *w/v* unless otherwise mentioned.

Transmission electron microscopy (TEM). 10 μL of hydrogel samples were drop cast in a 400-mesh copper grid covered by a carbon-stabilized Formvar film (SPI, West Chester, PA, USA). The samples were dried under ambient conditions. The TEM images were captured using a JEM-1400Plus Transmission Electron Microscope at 80 kV.

Fluorescence spectroscopy. Fluorescence study of the peptide hydrogel at different concentrations was carried out in a Horiba Jobin Yvon spectrofluorometer instrument. Each gel sample was prepared in a screw-capped quartz cell of 1 cm path length and was excited at 280 nm. The emission scans were recorded from 290 to 550 nm using a slit width of 3 nm with a 1 nm wavelength increment having an integration time of 0.1 s.

Fourier-transform infrared (FTIR). The FTIR spectra of the dried peptide and hybrid hydrogels were recorded using KBr pellets in Bruker alpha FTIR spectrometer.

Circular dichroism (CD). Fmoc-Lys(Fmoc)-Phe assemblies at 0.01% *w/v* was prepared in a screw-capped quartz cell of 1 mm path length. Circular dichroism study of the assemblies was carried out in a Jasco J-815 CD spectrometer.

X-ray diffraction (XRD). The hydrogel was drop cast on a glass slide, and the measurements were carried out on a Bruker Discover D8 X-ray diffractometer with Cu-Kα as the source.

Rheology. The mechanical properties of the hydrogels at different concentrations were measured using a 20 mm parallel-plate geometry with a gap of 1000 μm on an ARES-G2 rheometer (TA Instruments, New Castle, DE, USA). The sheer recovery test was done by the step strain method, with time sweep steps successively carried out at 0.1% and 200% strain. The mechanical properties of the composite hydrogel were performed on a Malvern rheometer using a 20 mm parallel-plate geometry with a gap of 300 μm.

Differential scanning calorimetry (DSC). The melting temperature of the peptide gel was determined using a differential scanning calorimeter (TA Instruments DSC Q200). The peptide gel sample was taken in large-volume stainless steel capsules fitted with O-rings and was equilibrated at 10°C for 10 min. They were heated at the heating rate of 5°C min^{-1} to 90°C under a nitrogen atmosphere. The melting point of the sample was determined from the peak position of the endotherm.

Raman spectroscopy. The dispersed solution of edge-functionalized GO and composite hydrogel samples were drop-casted on a glass slide and dried adequately. Raman scan was performed from 1000 – 3000 cm^{-1} in a WITec alpha 300 instrument using a laser light of 532 nm and grating of 600 g mm^{-1}.

Electrical Properties. Electrical conduction in the composite gel was investigated from their *I–V* characteristics. The data was gathered in the LSV mode by sandwiching the sample between two stainless steel electrodes over the voltage range −1 to +1 V at a scan rate of 10 mV s^{-1}. The impedance measurements of the dried composite hydrogels were carried at 25°C over the frequency range from 1kHz - 1MHz. The ac perturbation was 10 mV at 0 V DC level. Cyclic Voltametry (CV) measurements were taken by drop casting the composite

hydrogel on FTO plates and drying. The measurements were performed in a three-electrode cell with 6 M KOH aqueous electrolyte.

Molecular dynamics.

Coarse-grained models of Fmoc-Lys(Fmoc)-Phe, DMSO, and water molecules.

The Fmoc-Lys(Fmoc)-Phe molecule is modeled using the coarse-grained Martini model (version 2.1),[1] in which each bead represents 2~4 heavy atoms. The mapping from all-atom models to coarse-grained models is shown in Figure 6a-b. Both bonded and non-bonded parameters for the Lys and Phe residues are obtained from the Martini protein model,[2] and the parameters for the Fmoc protection group is taken from our previous work.[3,4] The coarse-grained model and force field parameters for the DMSO molecules are taken from our previous work.[5] The water molecules are modeled using the Martini P4 bead.

Coarse-grained simulations.

All simulations are performed using the GROMACS package (version 2018.3)[6] on a high-performance GPU cluster. Electrostatic interactions are treated using the reaction field method,[7] with a cutoff of 1.2 nm. The vdW interactions are calculated using a cutoff of 1.2 nm. The solute and solvent are separately coupled to an external temperature bath using a velocity rescaling method[8] and a pressure bath using the Parrinello-Rahman method.[9] The temperature and pressure are maintained at 300 K and 1 bar, respectively. The neighbor-list is updated every 10 steps with a cut-off distance of 1.2 nm using a Verlet buffer.

Trajectory analysis.

The trajectory analyses are performed using our in-house codes and tools implemented in the GROMACS package. The SASA is calculated using the Shrake-Rupley algorithm[10] with the van der Waals probe size set as 0.264 nm for regular coarse-grained beads and 0.230 nm for beads in aromatic rings.[1] The normalized SASA is calculated by dividing the molecules' SASA by their SASA at the initial randomly dispersed state. The SASA proportion of a group is calculated by dividing its SASA by the total SASA of the aggregate. Two peptide molecules (or two groups) are considered to have molecular contacts if their minimum distance is less than 0.6 nm. In accordance with our recent study,[11] the self-assembly of Fmoc-Lys(Fmoc)-Phe molecule is characterized using collapse degree and clustering degree. Collapse degree is defined as the ratio of SASA of all Fmoc-Lys(Fmoc)-Phe molecules in the initial state to their SASA in the final configuration.[12] Clustering degree is defined by molecules in clusters divided by the total number of molecules in the system.[11] The free energy surface of aromatic stacking interactions is calculated using $F=-RT\ln P(r, \theta)$, where $P(r, \theta)$ refers to the probability

of two aromatic rings have a specific centroid distance r and angle θ. All snapshots and illustrations are rendered using the PyMOL package.[13]

Table S1: Values of G′ and G″ at different peptide concentrations.

Concentration of Peptide	Value of G′ at 0.1% strain	Value of G″ at 0.1% strain
0.1% w/*v*	1529	280
0.25% w/*v*	4858	470
0.5% w/*v*	19710	1577
1% w/*v*	7107	522

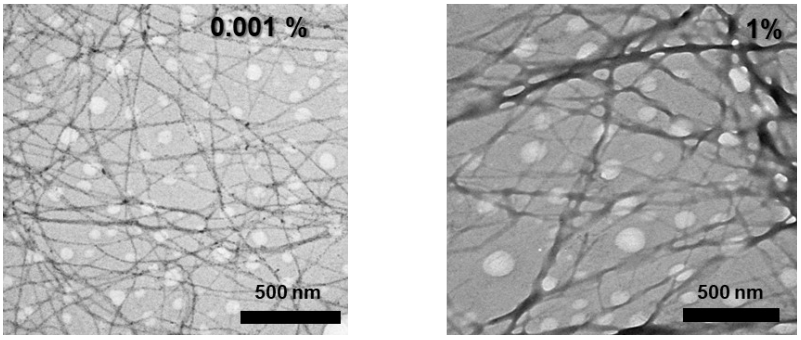

Figure S1. TEM images of the peptide hydrogel/assemblies at 0.001% *w/v* and 1% *w/v*.

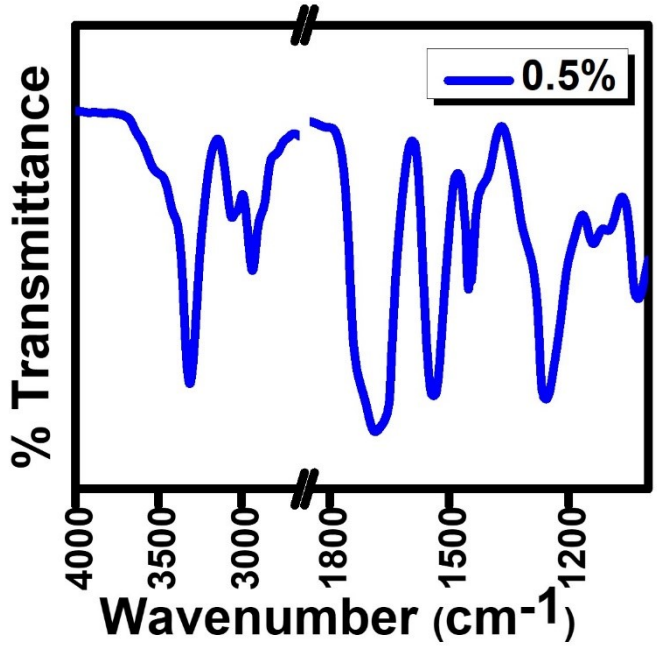

Figure S2. FTIR spectra (full region) of dried peptide hydrogel.

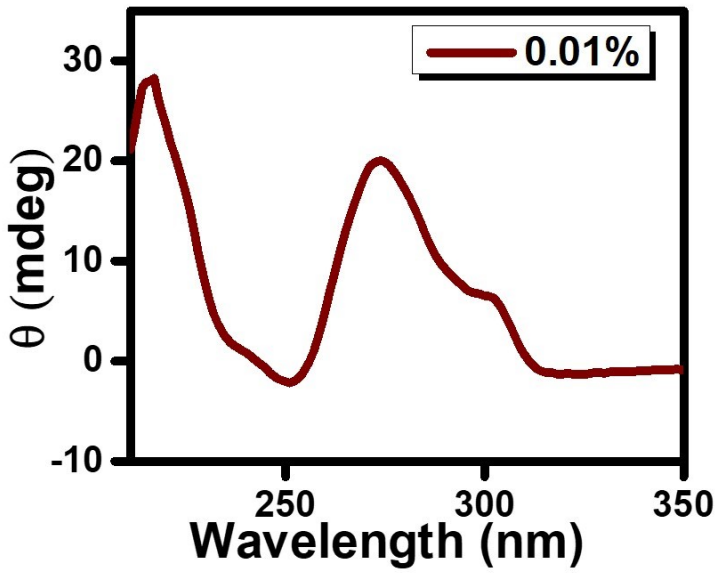

Figure S3. CD spectra of the peptide assembly at 0.01% *w/v*.

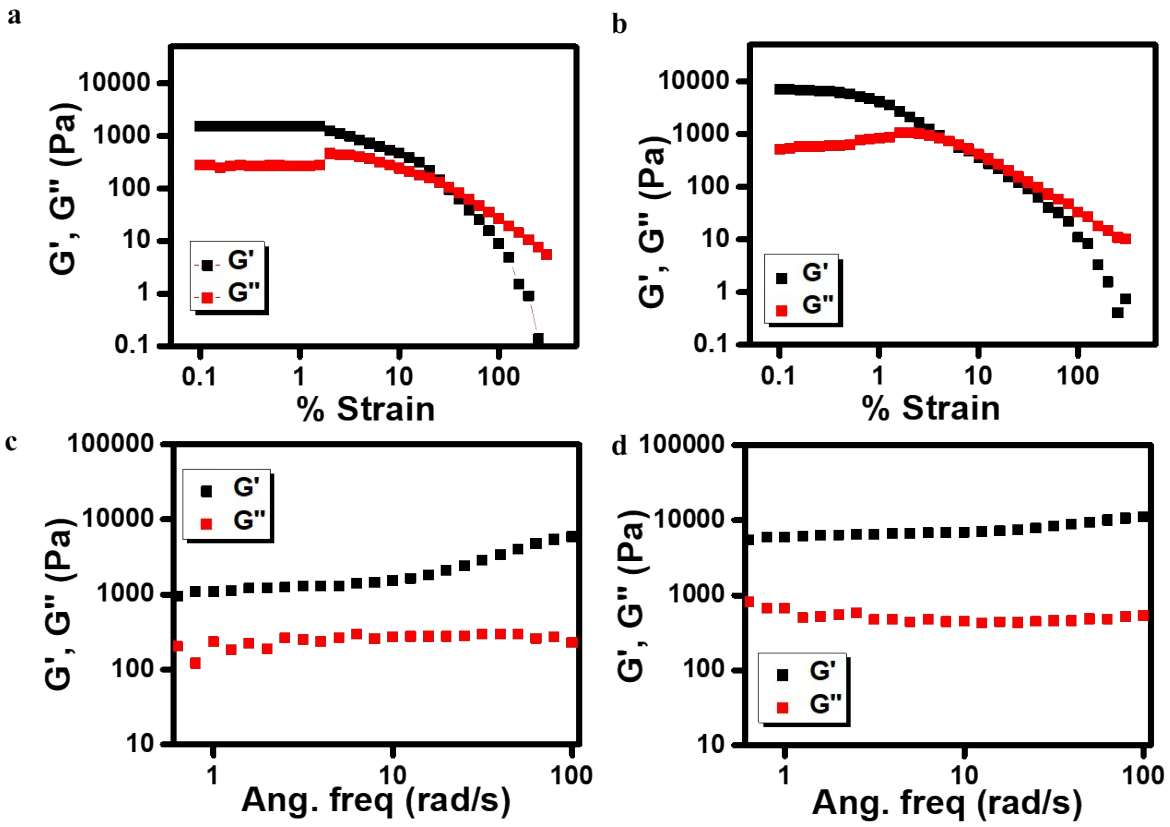

Figure S4. Strain sweep experiment carried out on the hydrogels at (a) 0.1% *w/v*, (b) 1% *w/v* concentrations. Frequency-dependent oscillatory rheology at 0.1% strain of the hydrogels at (c) 0.1% *w/v* and (d) 1% *w/v* concentration.

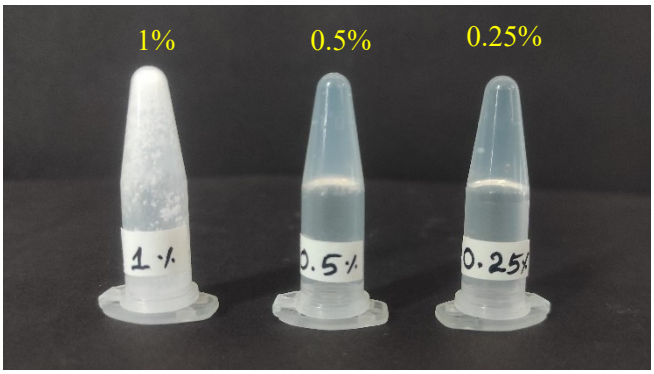

Figure S5. The self-assembly and gelation behaviour of the peptide (1%, 0.5%, 0.25% *w/v*) at a constant ϕDMSO/H_2O ratio (0.1).

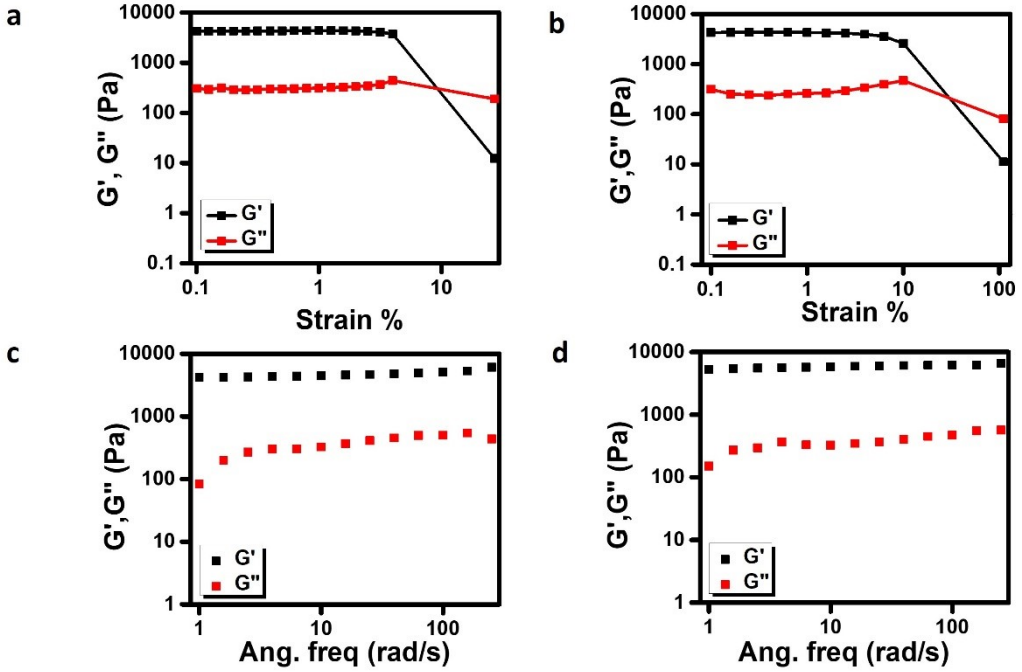

***Figure S6*. Mechanical properties of the peptide hydrogels at 0.25% and 0.5% (10% *v/v*, ϕDMSO/H_2O = 0.1).** Strain sweep experiment was carried out on the peptide hydrogel at of (a) 0.25% *w/v*, and (b) 0.5% *w/v* concentrations. Frequency-dependent oscillatory rheology of the peptide hydrogel at (c) 0.25% *w/v*, (d) 0.5% *w/v* concentrations (0.5% strain).

Supporting Note 1.

Moreover, we studied the mechanical properties of the peptide hydrogels at different concentrations while keeping the DMSO concentration constant (10% *v/v*, ϕDMSO/H_2O = 0.1). We prepared the peptide hydrogels at different concentrations (0.25%, 0.5%, and 1% w/v) while keeping the ϕDMSO/H_2O constant (0.1). Interestingly, while the peptide produced stable hydrogels at 0.25% and 0.5% concentrations, the 1% concentration failed to form a hydrogel, probably due to the insolubility of the peptide (**Figure S5**). We have further performed the rheological characterizations of the 0.25% and the 0.5% hydrogels (**Figure S6**). Strain sweep experiments reveal that 0.25% and 0.5% hydrogels exhibited a breakage strain at 9% and 31%, respectively (**Figure S6**). Dynamic frequency sweep experiments exhibited a wide linear viscoelastic region for both the concentrations with G'>G". The 0.25% and 0.5% hydrogels showed G' values of 4200 and 5256 Pa (at 1 rad/s). The 0.5% hydrogel at 10% DMSO evidently exhibits a lower G' value (5256 Pa) compared to the hydrogel at 7% DMSO at the same peptide concentration (19710 Pa). This decrease might result from the increased DMSO in the formulation that causes a higher peptide solubility, thus lowering the intermolecular interactions required for self-assembly.

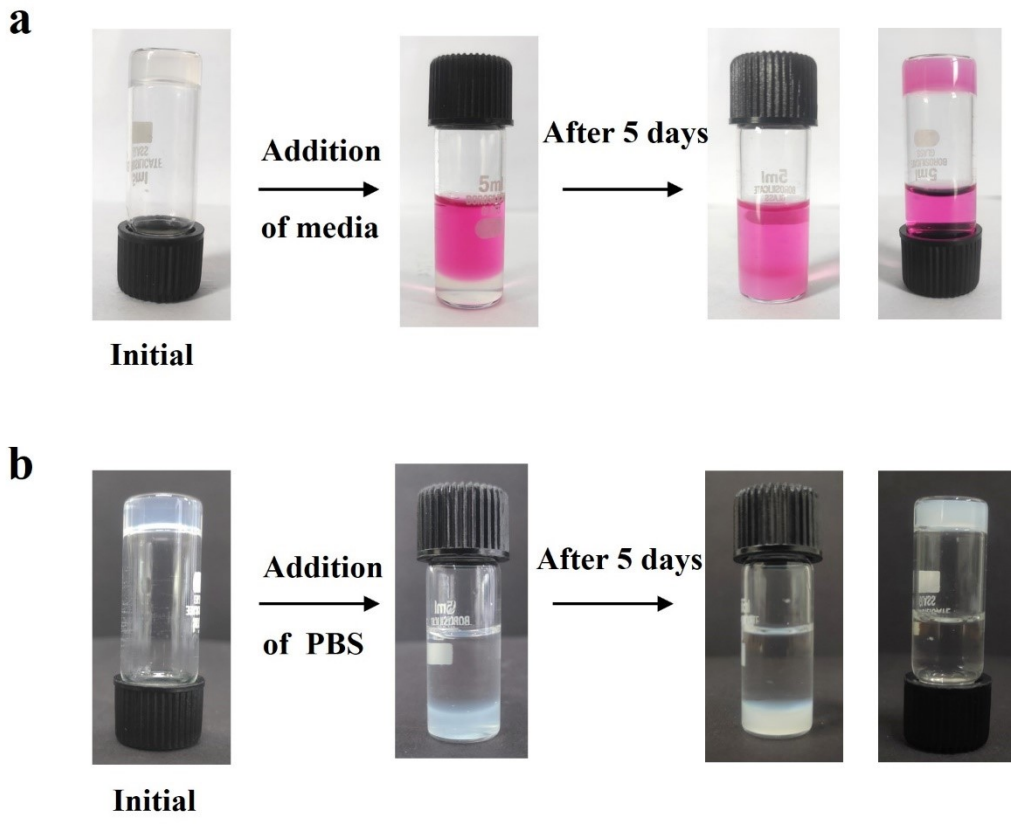

***Figure S7*: Stability of peptide hydrogels (0.5% *w/v*)** in (a) cell culture media (DMEM with high glucose), (b) PBS (1X)

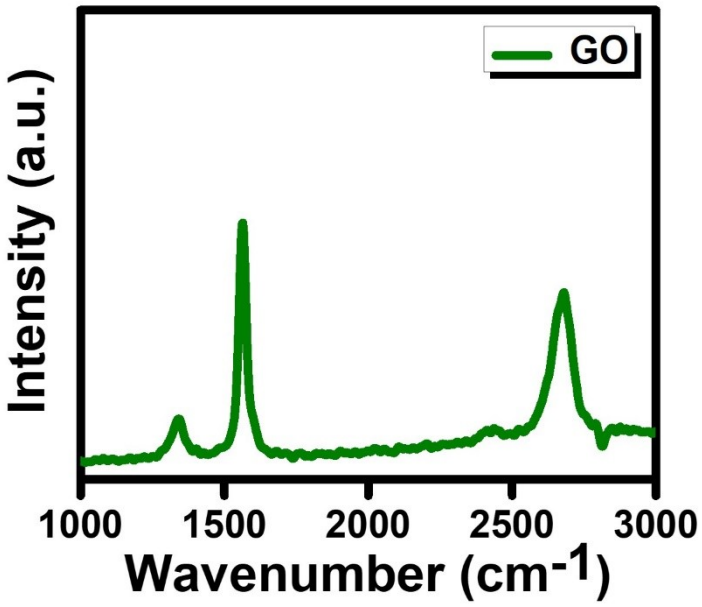

Figure S8. Raman spectrum of edge functionalized GO.

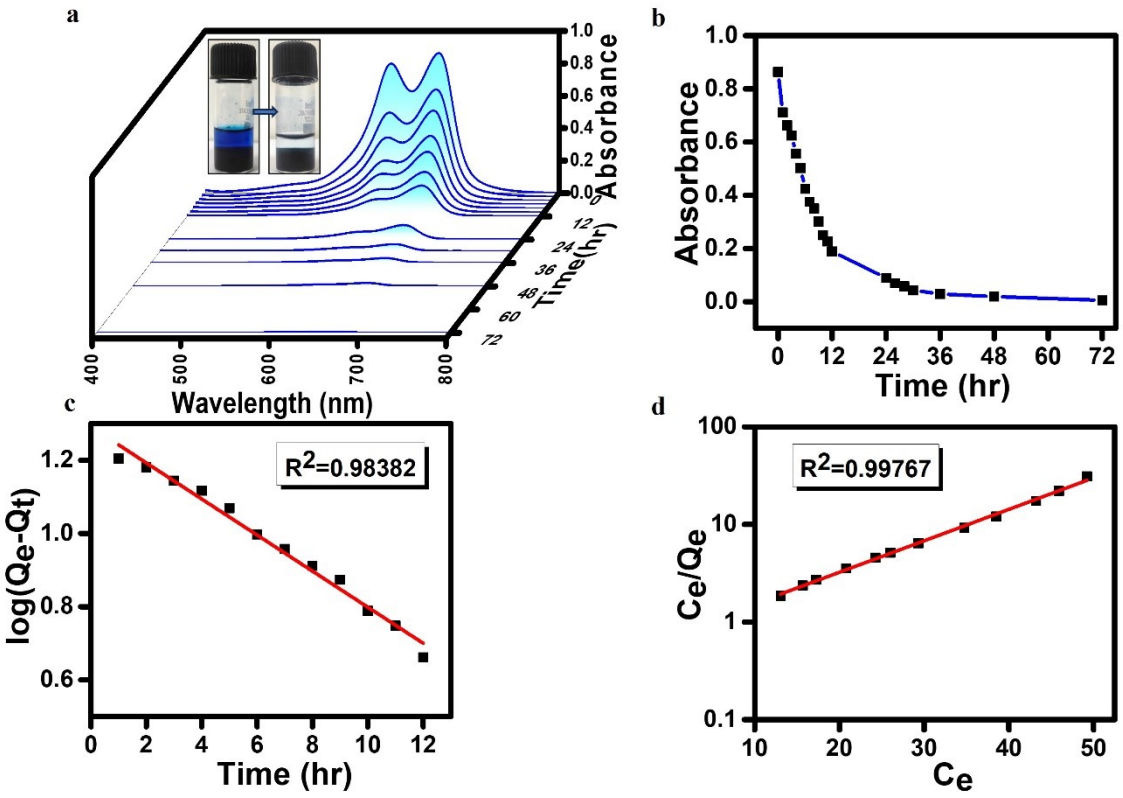

Figure S9. a) UV-vis study of MB on composite hydrogel sampling the supernatant at different time intervals. b) Variation of absorbance with time. c) Pseudo first order kinetics plot of MB dye. d) Langmuir isotherm for MB on composite hydrogel at 25°C.

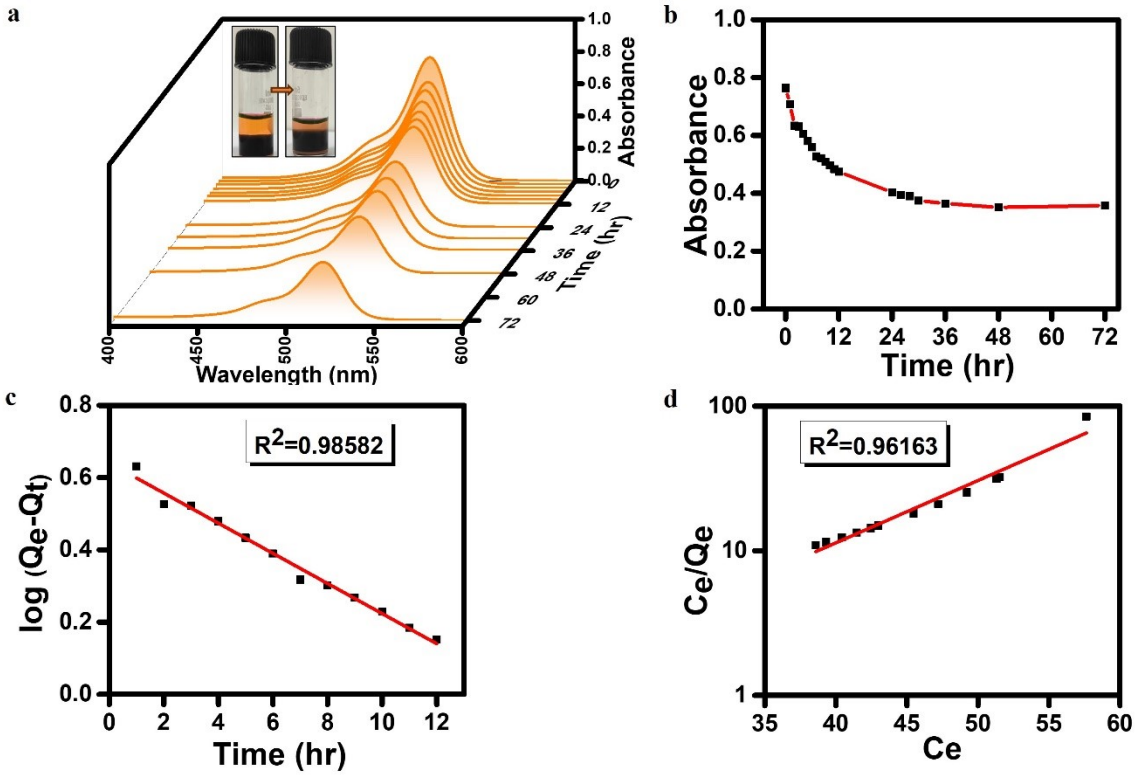

Figure S10. a) UV-vis study of EY on composite hydrogel sampling the supernatant at different time intervals. b) Variation of absorbance with time c) Pseudo first order kinetics plot of EY dye. d) Langmuir isotherm for EY on composite hydrogel at 25°C.

References:

[1] S. J. Marrink, H. J. Risselada, S. Yefimov, D. P. Tieleman, A. H. de Vries, *J Phys Chem B* **2007**, *111*, 7812–7824.

[2] L. Monticelli, S. K. Kandasamy, X. Periole, R. G. Larson, D. P. Tieleman, S.-J. Marrink, *J Chem Theory Comput* **2008**, *4*, 819–834.

[3] P. Chakraborty, Y. Tang, T. Guterman, Z. A. Arnon, Y. Yao, G. Wei, E. Gazit, *Angew Chem* **2020**, *132*, 23939–23947.

[4] V. Basavalingappa, T. Guterman, Y. Tang, S. Nir, J. Lei, P. Chakraborty, L. Schnaider, M. Reches, G. Wei, E. Gazit, *Adv Sci* **2019**, *6*, 1900218.

[5] W. Ji, Y. Tang, P. Makam, Y. Yao, R. Jiao, K. Cai, G. Wei, E. Gazit, *J Am Chem Soc* **2021**, *143*, 17633–17645.

[6] D. Van Der Spoel, E. Lindahl, B. Hess, G. Groenhof, A. E. Mark, H. J. C. Berendsen, *J Comput Chem* **2005**, *26*, 1701–1718.

[7] I. G. Tironi, R. Sperb, P. E. Smith, W. F. van Gunsteren, *J Chem Phys* **1995**, *102*, 5451–5459.

[8] G. Bussi, D. Donadio, M. Parrinello, *J Chem Phys* **2007**, *126*, 014101.

[9] M. Parrinello, A. Rahman, *J Appl Phys* **1981**, *52*, 7182–7190.

[10] A. Shrake, J. A. Rupley, *J Mol Biol* **1973**, *79*, 351–371.

[11] Y. Tang, S. Bera, Y. Yao, J. Zeng, Z. Lao, X. Dong, E. Gazit, G. Wei, *Cell Rep Phys Sci* **2021**, *2*, 100579.

[12] P. W. J. M. Frederix, G. G. Scott, Y. M. Abul-Haija, D. Kalafatovic, C. G. Pappas, N. Javid, N. T. Hunt, R. V. Ulijn, T. Tuttle, *Nat Chem* **2015**, *7*, 30–37.

[13] L. Schrödinger, The PyMOL Molecular Graphics System. **2015**.